We are IntechOpen, the world's leading publisher of Open Access books Built by scientists, for scientists

4,800
Open access books available

122,000
International authors and editors

135M
Downloads

Our authors are among the

154
Countries delivered to

TOP 1%
most cited scientists

12.2%
Contributors from top 500 universities

CLARIVATE ANALYTICS BOOK CITATION INDEX INDEXED

WEB OF SCIENCE™

Selection of our books indexed in the Book Citation Index in Web of Science™ Core Collection (BKCI)

Interested in publishing with us?
Contact book.department@intechopen.com

Numbers displayed above are based on latest data collected.
For more information visit www.intechopen.com

5

Electromagnetic Wave Propagation in Two-Dimensional Photonic Crystals

Oleg L. Berman[1], Vladimir S. Boyko[1],
Roman Ya. Kezerashvili[1,2] and Yurii E. Lozovik[3]
[1]*Physics Department, New York City College of Technology, The City University of New York, Brooklyn, NY 11201*
[2]*The Graduate School and University Center, The City University of New York, New York, NY 10016*
[3]*Institute of Spectroscopy, Russian Academy of Sciences, 142190 Troitsk*
[1,2]*USA*
[3]*Russia*

1. Introduction

Photonic crystals are media with a spatially periodical dielectric function (Yablonovitch, 1987; John, 1987; Joannopoulos et al., 1995; 2008). This periodicity can be achieved by embedding a periodic array of constituent elements with dielectric constant ε_1 in a background medium characterized by dielectric constant ε_2. Photonic crystals were first discussed by Yablonovitch (Yablonovitch, 1987) and John (John, 1987). Different materials have been used for the corresponding constituent elements including dielectrics (Joannopoulos et al., 1995; 2008), semiconductors, metals (McGurn & Maradudin, 1993; Kuzmiak & Maradudin, 1997), and superconductors (Takeda & Yoshino, 2003; Takeda et al., 2004; Berman et al., 2006; Lozovik et al., 2007; Berman et al., 2008; 2009). Photonic crystals attract the growing interest due to various modern applications (Chigrin & Sotomayor Torres, 2003). For example, they can be used as the frequency filters and waveguides (Joannopoulos et al., 2008).

The photonic band gap (PBG) in photonic crystals was derived from studies of electromagnetic waves in periodic media. The idea of band gap originates from solid-state physics. There are analogies between conventional crystals and photonic crystals. Normal crystals have a periodic structure at the atomic level, which creates periodic potentials for electrons with the same modulation. In photonic crystals, the dielectrics are periodically arranged and the propagation of photons is largely affected by the structure. The properties of the photons in the photonic crystals have the common properties with the electrons in the conventional crystals, since the wave equations in the medium with the periodic dielectric constant have the band spectrum and the Bloch wave solution similarly to the electrons described by the Schrödinger equation with the periodic potential (see (Berman et al., 2006) and references therein). Photonic crystals can be either one-, two- or three-dimensional as shown in Fig. 1.

In normal crystals there are valence and conduction bands due to the periodic field. Electrons cannot move inside the completely filled valence band due to the Pauli exclusion principle for electrons as fermions. Electrons can move inside the crystal if they are excited to the

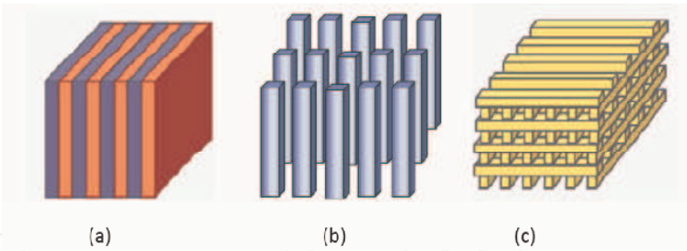

Fig. 1. Example of 1D, 2D and 3D photonic crystals. All of the photonic crystals shown above have two different dielectric media. (a) 1D multilayer; (b) 2D array of dielectric rods; (c) 3D woodpile.

conduction band. Because the photons are bosons, all bands in the photonic crystals' band structure are conduction bands. If the frequency corresponds to the allowed band, the photon can travel through the media. If the photonic gap exists only in the part of Brillouin zone, then this gap corresponds to the stop band. By other words, photons cannot propagate with frequencies inside the gap at the wavevectors, where this gap exists. Of particular interest is a photonic crystal whose band structure possesses a complete photonic band gap. A PBG defines a range of frequencies for which light is forbidden to exist inside the crystal.

The photonic crystals with the dielectric, metallic, semiconductor, and superconducting constituent elements have different photonic band and transmittance spectra. The dissipation of the electromagnetic wave in all these photonic crystals is different. The photonic crystals with the metallic and superconducting constituent elements can be used as the frequency filters and waveguides for the far infrared region of the spectrum, while the dielectric photonic crystals can be applied for the devices only for the optical region of the spectrum.

In this Chapter we discuss the photonic band structure of two-dimensional (2D) photonic crystals formed by dielectric, metallic, and superconducting constituent elements and graphene layers. The Chapter is organized in the following way. In Sec. 2 we present the description of 2D dielectric photonic crystals. In Sec. 3 we review the 2D photonic crystals with metallic and semiconductor constituent elements. In Sec. 4 we consider the photonic band structure of the photonic crystals with the superconducting constituents. A novel type of the graphene-based photonic crystal formed by embedding a periodic array of constituent stacks of alternating graphene and dielectric discs into a background dielectric medium is studied in Sec. 5. Finally, the discussion of the results presented in this Chapter follows in Sec. 6.

2. Dielectric photonic crystals

The 2D photonic crystals with the dielectric constituent elements were discussed in Ref. (Joannopoulos et al., 2008). Maxwell's equations, in the absence of external currents and sources, result in a form which is reminiscent of the Schrödinger equation for magnetic field $\mathbf{H}(\mathbf{r})$ (Joannopoulos et al., 2008):

$$\nabla \times \left(\frac{1}{\varepsilon(\mathbf{r})} \nabla \times \mathbf{H}(\mathbf{r}) \right) = \left(\frac{\omega}{c} \right)^2 \mathbf{H}(\mathbf{r}) \,, \tag{1}$$

where ω is the frequency of the electromagnetic wave, c is the speed of light, $\varepsilon(\mathbf{r})$ is the dielectric constant, which is the periodic function of the radius vector in the photonic crystal. Eq. (1) represents a linear Hermitian eigenvalue problem whose solutions are determined entirely by the properties of the macroscopic dielectric function $\varepsilon(\mathbf{r})$. Therefore, for a crystal

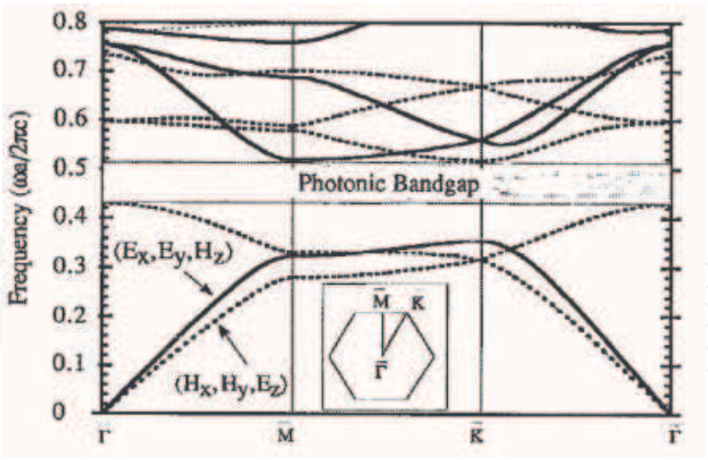

Fig. 2. Frequencies of the lowest photonic bands for a triangular lattice of air columns ($\varepsilon_{air} = 1$) drilled in dielectric ($\varepsilon = 13$). The band structure is plotted along special directions of the in-plane Brillouin zone ($k_z = 0$), as shown in the lower inset. The radius of the air columns is $r = 0.48a$, where a is the in-plane lattice constant. The solid (dashed) lines show the frequencies of bands which have the electric field parallel (perpendicular) to the plane. Notice the PBG between the third and fourth bands.

consisting of a periodic array of macroscopic uniform dielectric constituent elements, the photons in this photonic crystal could be described in terms of a band structure, as in the case of electrons. Of particular interest is a photonic crystal whose band structure possesses a complete photonic band gap.

All various kinds of 2D dielectric photonic crystals were analyzed including square, triangular, and honeycomb 2D lattices (Joannopoulos et al., 2008; Meade et al., 1992). Dielectric rods in air, as well as air columns drilled in dielectric were considered. At the dielectric contrast of GaAs ($\varepsilon = 13$), the only combination which was found to have a PBG in both polarizations was the triangular lattice of air columns in dielectric. Fig. 2 (Meade et al., 1992) represents the eigenvalues of the master equation (1) for a triangular lattice of air columns ($\varepsilon_{air} = 1$) drilled in dielectric ($\varepsilon = 13$).

The photonic band structure in a 2D dielectric array was investigated using the coherent microwave transient spectroscopy (COMITS) technique (Robertson et al., 1992). The array studied in (Robertson et al., 1992) consists of alumina-ceramic rods was arranged in a regular square lattice. The dispersion relation for electromagnetic waves in this photonic crystal was determined directly using the phase sensitivity of COMITS. The dielectric photonic crystals can be applied as the frequency filters for the optical region of spectrum, since the propagation of light is forbidden in the photonic crystal at the frequencies, corresponding to the PBG, which corresponds to the optical frequencies.

3. Photonic crystals with metallic and semiconductor components

The photonic band structures of a square lattice array of metal or semiconductor cylinders, and of a face centered cubic lattices array of metal or semiconductor spheres, were studies in Refs. (McGurn & Maradudin, 1993; Kuzmiak & Maradudin, 1997). The frequency-dependent dielectric function of the metal or semiconductor is assumed to have the free-electron Drude form $\varepsilon(\omega) = 1 - \omega_p^2/\omega^2$, where ω_p is the plasma frequency of the charge carriers. A

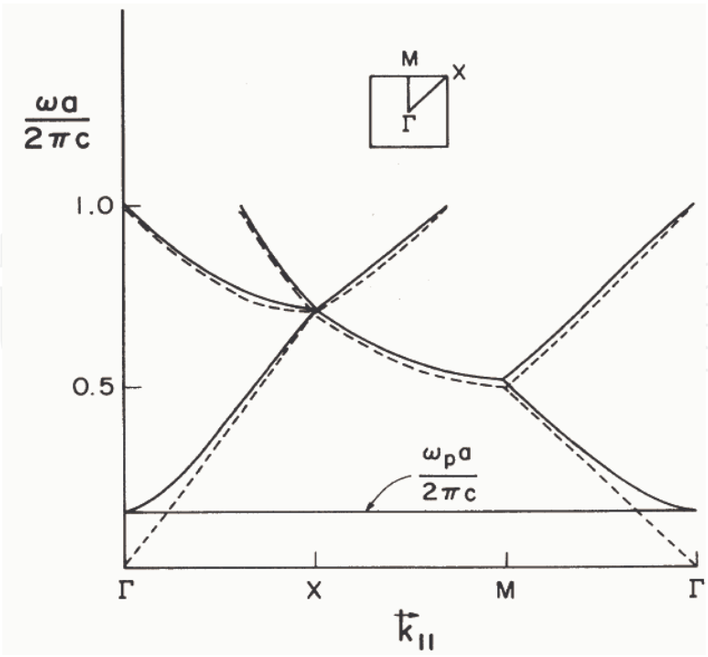

Fig. 3. Band structure for a square lattice of metal cylinders with a filling factor $f = 70\%$. Only results for $\omega \geq \omega_p$ are shown. Results for the dispersion curve in vacuum are shown as dashed lines.

plane-wave expansion is used to transform the vector electromagnetic wave equation into a matrix equation. The frequencies of the electromagnetic modes are found as the zeros of the determinant of the matrix.

The results of the numerical calculations of the photonic band structure for 2D photonic crystal formed by a square lattice of metal cylinders with a filling factor $f = 70\%$ are shown in Fig. 3 (McGurn & Maradudin, 1993). Here the filling factor f is defined as $f \equiv S_{cyl}/S = \pi r_0^2/a^2$, where S_{cyl} is the cross-sectional area of the cylinder in the plane perpendicular to the cylinder axis, S is the total area occupied by the real space unit cell, and r_0 is the cylinder radius.

The photonic crystals with the metallic and semiconductor constituent elements can be used as the frequency filters and waveguides for the far infrared range of spectrum, since the PBG in these photonic crystals corresponds to the frequencies in the far infrared range (McGurn & Maradudin, 1993; Kuzmiak & Maradudin, 1997).

Photonic gaps are formed at frequencies ω at which the dielectric contrast $\omega^2(\varepsilon_1(\omega) - \varepsilon_2(\omega))$ is sufficiently large. Since the quantity $\omega^2\varepsilon(\omega)$ enters in the electromagnetic wave equation (Joannopoulos et al., 1995; 2008), only metal-containing photonic crystals can maintain the necessary dielectric contrast at small frequencies due to their Drude-like behavior $\varepsilon_{Met}(\omega) \sim -1/\omega^2$ (McGurn & Maradudin, 1993; Kuzmiak & Maradudin, 1997). However, the damping of electromagnetic waves in metals due to the skin effect (Abrikosov, 1988) can suppress many potentially useful properties of metallic photonic crystals.

4. Superconducting photonic crystals

4.1 Photonic band structure of superconducting photonic crystals

Photonic crystals consisting of superconducting elements embedded in a dielectric medium was studied in Ref. (Berman et al., 2006). The equation for the electric field in the ideal lattice of parallel cylinders embedded in medium has the form (Berman et al., 2009)

$$-\nabla^2 E_z(x,y) = \frac{\omega^2}{c^2}\left[\Lambda \pm (\varepsilon(\omega)-\epsilon)\sum_{\{\mathbf{n}^{(l)}\}}\eta(\mathbf{r}\in S)\right]E_z(x,y)\,, \tag{2}$$

where ϵ is the dielectric constant of dielectric, $\varepsilon(\omega)$ is a dielectric function of the superconductor component. This equation describes the electric field in the ideal lattice of parallel superconducting cylinders (SCCs) in dielectric medium (DM) when within brackets on the right side is taken $\Lambda = \epsilon$ and sign "+" and the electric field in the ideal lattice of parallel DCs cylinders in a superconducting medium when $\Lambda = \varepsilon(\omega)$ and sign "-". In Eq. (2) $\eta(\mathbf{r}\in S)$ is the Heaviside step function. $\eta(\mathbf{r}\in S)=1$ if $\mathbf{r}$ is inside of the cylinders S, and otherwise $\eta(\mathbf{r}\in S)=0$, $\mathbf{n}^{(l)}$ is a vector of integers that gives the location of scatterer l at $\mathbf{a}(\mathbf{n}^{(l)}) \equiv \sum_{i=1}^{d} n_i^{(l)}\mathbf{a}_i$ ($\mathbf{a}_i$ are real space lattice vectors and d is the dimension of the lattice). The summation in Eq. (2) goes over all lattice nodes characterizing positions of cylinders. Eq. (2) describes the lattice of parallel cylinders as the two-component 2D photonic crystal. The first term within the bracket is associated to the medium, while the second one is related to the cylinders. Here and below the system described by Eq. (2) will be defined as an ideal photonic crystal. The ideal photonic crystal based on the 2D square lattice of the parallel superconducting cylinders was studied in Refs. (Berman et al., 2006; Lozovik et al., 2007).

Let us describe the dielectric constant for the system superconductor-dielectric. We describe the dielectric function of the superconductor within the Kazimir–Gorther model (Lozovik et al., 2007). In the framework of this model, it is assumed that far from the critical temperature point of the superconducting transition there are two independent carrier liquids inside a superconductor: superconducting with density $n_s(T,B)$ and normal one with density $n_n(T,B)$. The total density of electrons is given by $n_{tot} = n_n(T,B) + n_s(T,B)$. The density of the superfluid component $n_s(T,B)$ drops and the density of the normal component $n_n(T,B)$ grows when the temperature T or magnetic field B increases. The dielectric function in the Kazimir-Gorther model of superconductor is defined as

$$\varepsilon(\omega) = 1 - \frac{\omega_{ps}^2}{\omega^2} - \frac{\omega_{pn}^2}{\omega(\omega+i\gamma)}\,, \tag{3}$$

where ω is the frequency and γ represents the damping parameter in the normal conducting states. In Eq. (1) ω_{ps} and ω_{pn} are the plasma frequencies of superconducting and normal conducting electrons, respectively and defined as

$$\omega_{pn} = \left(\frac{4\pi n_n e^2}{m}\right)^{1/2}, \quad \omega_{ps} = \left(\frac{4\pi n_s e^2}{m}\right)^{1/2}, \tag{4}$$

where m and e are the mass and charge of an electron, respectively. The plasma frequency ω_{p0} is given by

$$\omega_{p0} = \left(\frac{4\pi n_{tot} e^2}{m}\right)^{1/2}. \tag{5}$$

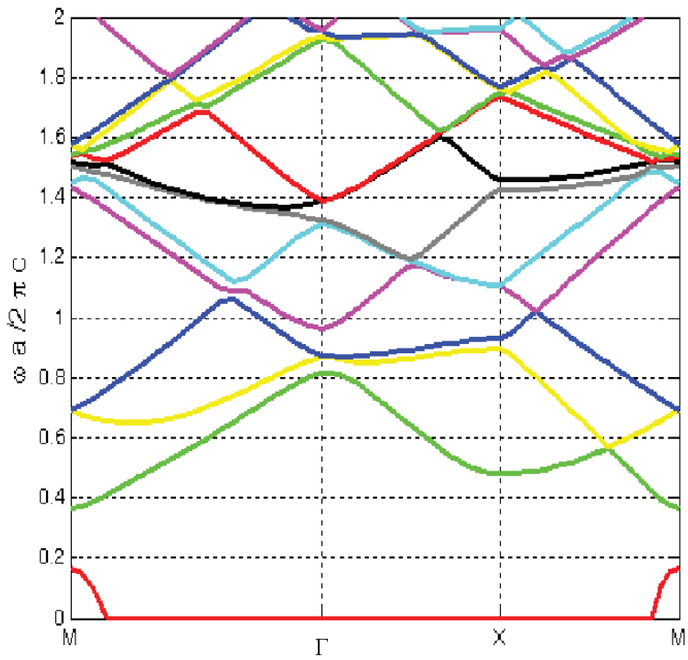

Fig. 4. Dispersion relation for a 2D photonic crystal consisting of a square lattice of parallel infinite superconducting cylinders with the filling factor $f = 0.3$. The ordinate plots frequencies in lattice units $2\pi c/a$. A band gap is clearly apparent in the frequency range $0.18 < \omega < 0.38$ in units of $2\pi c/a$.

From Eqs. (4) and (5) it is obvious that

$$\omega_{p0}^2 = \omega_{ps}^2 + \omega_{pn}^2 \, . \tag{6}$$

For the such superconductor, when the condition $\gamma \ll \omega_{p0}$ is valid, the damping parameter in the dielectric function can be neglected. Therefore, taking into account Eq. (6), Eq. (3) can be reduced to the following expression

$$\varepsilon(\omega) = 1 - \frac{\omega_{p0}^2}{\omega^2} \, . \tag{7}$$

Thus, Eq. (7) defines the dependence of the dielectric function of the superconductor on the frequency.

The photonic band structure for a 2D photonic crystal consisting of a square lattice of parallel infinite superconducting cylinders in vacuum was calculated using the eigenfrequencies of Eq. (2) obtained by the plane wave expansion method (Berman et al., 2006). The dielectric function of the superconductor $\varepsilon(\omega)$ in Eq. (2) was substituted from Eq. (7). The photonic band structure of the photonic crystal build up from the $YBa_2Cu_3O_{7-\delta}$ (YBCO) superconducting cylinders embedded in vacuum is presented in Fig. 4. Since for the YBCO the plasma frequency $\omega_{p0} = 1.67 \times 10^{15}$rad/s and the damping parameter $\gamma = 1.84 \times 10^{13}$rad/s, then the condition $\gamma \ll \omega_{p0}$ is valid for the YBCO superconductor, and Eq. (7) can used for the dielectric function of the YBCO superconductor.

The advantage of a photonic crystal with superconducting constituents is that the dissipation of the incident electromagnetic wave due to the imaginary part of the dielectric function

is much less than for normal metallic constituents at frequencies smaller than the superconducting gap. Thus, in this frequency regime, for a photonic crystal consisting of several layers of scatterers the dissipation of the incident electromagnetic wave by an array of superconducting constituents is expected to be less than that associated with an analogous array composed of normal metallic constituents.

4.2 Monochromatic infrared wave propagation in 2D superconductor-dielectric photonic crystal

The dielectric function in the ideal photonic crystal is a spatially periodic. This periodicity can be achieved by the symmetry of a periodic array of constituent elements with one kind of the dielectric constant embedded in a background medium characterized by the other kind of the dielectric constant. The localized photonic mode can be achieved in the photonic crystals whose symmetry is broken by a defect (Yablonovitch et al., 1991; Meade et al., 1991; McCall et al., 1991; Meade et al., 1993). There are at least two ways to break up this symmetry: (i) to remove one constituent element from the node of the photonic crystal ("vacancy"); (ii) to insert one extra constituent element placed out of the node of photonic crystal ("interstitial"). We consider two types of 2D photonic crystals: the periodical system of parallel SCC in dielectric medium and the periodical system of parallel dielectric cylinders (DC) in superconducting medium. The symmetry of the SCCs in DM can be broken by two ways: (i) to remove one SCC out of the node, and (ii) to insert one extra SCC in DM out of the node. We will show below that only the first way of breaking symmetry results in the localized photonic state with the frequency inside the band gap for the SCCs in the DM. The second way does not result in the localized photonic state inside the band gap. The symmetry of DCs in SCM can be broken also by two ways: (i) to remove one DC out of the node, and (ii) to insert one extra DC in SCM out of the node. We will show below that only the second way of breaking symmetry results in the localized photonic state inside the band gap for DCs in SCM. The first way does not result in the localized photonic state.

Let us consider now the real photonic crystal when one SCC of the radius ξ removed from the node of the square lattice located at the position $\mathbf{r}_0$ or one extra DC of the same radius is placed out of the node of the square lattice located at the position $\mathbf{r}_0$ presented in Fig. 5. The free space in the lattice corresponding to the removed SCC in DM or to placed the extra DC in SCM contributes to the dielectric contrast by the adding the term $-(\varepsilon(\omega)-\epsilon)\eta(\xi-|\mathbf{r}-\mathbf{r}_0|)E_z(x,y)$ to the right-hand side in Eq. (2):

$$-\nabla^2 E_z(x,y)=\frac{\omega^2}{c^2}\left[\Lambda\pm(\varepsilon(\omega)-\epsilon)\sum_{\{\mathbf{n}^{(l)}\}}\eta(\mathbf{r}\in S)-(\varepsilon(\omega)-\epsilon)\eta(\xi-|\mathbf{r}-\mathbf{r}_0|)\right]E_z(x,y)\,, \quad (8)$$

Eq. (8) describes the photonic crystal implying a removed SCC from the node of the lattice ($\Lambda=\epsilon$ and sign "+") shown in Fig. 5a or implying the extra DC inserted and placed out of the node of the lattice ($\Lambda=\varepsilon(\omega)$ and sign "-") shown in Fig. 5b, which are defined as a real photonic crystal.

Substituting Eq. (7) into Eq. (8), we obtain for the wave equation for the real photonic crystal:

$$-\nabla^2 E_z(x,y)-\frac{\omega^2}{c^2}\left[\pm(1-\epsilon)\mp(\frac{\omega_{p0}^2}{\omega^2})\left(\sum_{\{\mathbf{n}^{(l)}\}}\eta(\mathbf{r}\in S)-\eta(\xi-|\mathbf{r}-\mathbf{r}_0|)\right)\right]E_z(x,y)=\Lambda\frac{\omega^2}{c^2}E_z(x,y)\,. \quad (9)$$

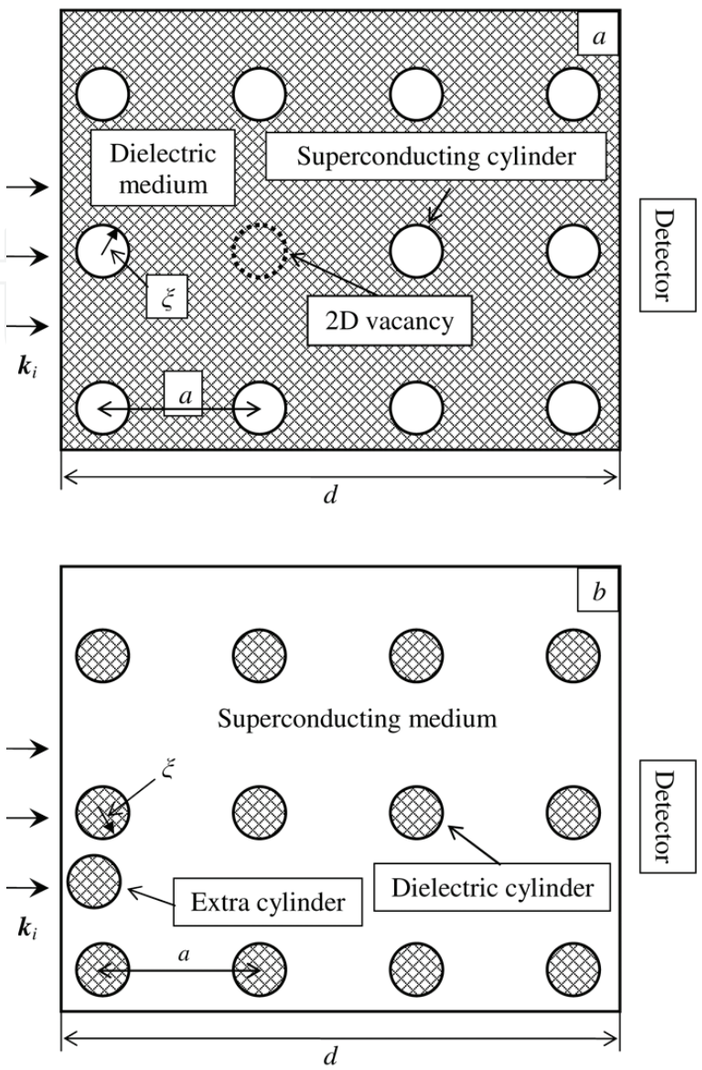

Fig. 5. Anomalous far infrared monochromatic transmission through a a lattice of (a) parallel SCCs embedded in DM and (b) parallel DCs embedded in SCM. a is the equilateral lattice spacing. ξ is the the radius of the cylinder. d denotes the length of the film. The dashed cylinder is removed out of the node of the lattice.

Follow Ref. (Berman et al., 2008) Eq. (9) can be mapped onto the Schrödinger equation for an "electron" with the effective electron mass in the periodic potential in the presence of the potential of the "impurity"Ṫherefore, the eigenvalue problem formulated by Eq. (9) can be solved in two steps: i. we recall the procedure of the solution the eigenvalue problem for the calculation of the photonic-band spectrum of the ideal superconducting photonic crystal (for SCCs in DM see Ref. (Berman et al., 2006; Lozovik et al., 2007)); ii. we apply the Kohn-Luttinger two-band model (Luttinger & Kohn, 1955; Kohn, 1957; Keldysh, 1964; Takhtamirov & Volkov, 1999) to calculate the eigenfrequency spectrum of the real photonic crystal with the symmetry broken by defect.

Eq. (9) when the dielectric is vacuum ($\epsilon = 1$) has the following form

$$-\nabla^2 E_z(x,y) + \left[\pm \frac{\omega_{p0}^2}{c^2} \sum_{\{\mathbf{n}^{(l)}\}} \eta(\mathbf{r} \in S) - \frac{\omega_{p0}^2}{c^2} \eta(\xi - |\mathbf{r} - \mathbf{r}_0|) \right] E_z(x,y) = \Lambda \frac{\omega^2}{c^2} E_z(x,y) \,. \quad (10)$$

In the framework of the Kohn-Luttinger two-band model the eigenvalue and localized eigenfunction of Eq. (10) are presented in Ref. (Berman et al., 2008). Since Eq. (10) is analogous to the wave equation for the electric field in Ref. (Berman et al., 2008), we can follow and apply the procedure of the solution of the eigenvalue problem formulated in Ref. (Berman et al., 2008) to the eigenvalue problem presented by Eq. (10). This procedure is reduced to the 2D Schrödinger-type equation for the particle in the negative potential given by step-function representing a 2D well. This equation has the localized eigenfunction representing the localized electric field as discussed in Ref. (Berman et al., 2008). Let us emphasize that this localized solution for the SCCs in DM can be obtained only if one cylinder is removed. If we insert the extra cylinder in 2D lattice of the SCCs, the corresponding wave equation will be represented by adding the term $(\varepsilon(\omega) - \epsilon)\eta(\xi - |\mathbf{r} - \mathbf{r}_0|)E_z(x,y)$ to the right-hand side of Eq. (2). This term results in the positive potential in the effective 2D Schrödinger-type equation. This positive potential does not lead to the localized eigenfunction. Therefore, inserting extra cylinder in the 2D ideal photonic crystal of the SCCs in DM does not result in the localized photonic mode causing the anomalous transmission.

In terms of the initial quantities of the superconducting photonic crystal the eigenfrequency ω of the localized photonic state is given by (Berman et al., 2008)

$$\omega = \left(\Delta^4 - A \right)^{1/4}, \quad (11)$$

where Δ is photonic band gap of the ideal superconducting photonic crystal calculated in Refs. (Berman et al., 2006; Lozovik et al., 2007) and A is given by

$$A = \frac{16 c^4 k_0^2}{3\xi^2} \exp\left[-\frac{8 k_0^2 c^4}{3\Delta^2 \xi^2 \omega_{p0}^2} \right] . \quad (12)$$

In Eq. (12) $k_0 = 2\pi/a$, where a is the period of the 2D square lattice of the SCCs. In the square lattice the radius of the cylinder ξ and the period of lattice a are related as $\xi = \sqrt{f/\pi}a$, where f is the filling factor of the superconductor defined as the ratio of the cross-sectional area of all superconducting cylinders in the plane perpendicular to the cylinder axis $S_{supercond}$ and the total area occupied by the real space unit cell S: $f \equiv S_{supercond}/S = \pi\xi^2/a^2$.

According to Refs. (Berman et al., 2006; Lozovik et al., 2007), the photonic band gap Δ for the ideal superconducting square photonic crystal at different temperatures and filling factors ($f = 0.3$ and $T = 0$ K, $f = 0.05$ and $T = 85$ K, $f = 0.05$ and $T = 10$ K) is given by $0.6c/a$ in Hz. The period of lattice in these calculations is given by $a = 150$ μm.

According to Eqs. (11) and (12), the eigenfrequency ν corresponding to the localized photonic mode for the parameters listed above for the YBCO is calculated as $\nu = \omega/(2\pi) = 117.3$ THz. The corresponding wavelength is given by $\lambda = 2.56 \times 10^{-6}$ m. Let us emphasize that the frequency corresponding to the localized mode does not depend on temperature and magnetic field at $\gamma \ll \omega_{p0}$, since in this limit we neglect damping parameter, and, according to Eq. (7), the dielectric constant depends only on ω_{p0}, which is determined by the total electron density n_{tot}, and n_{tot} does not depend on the temperature and magnetic field. Therefore, for given

parameters of the system at $f = 0.05$ the anomalous transmission appears at frequency $\nu =$ 117.3 THz inside the forbidden photonic gap $0 \leq \Delta/(2\pi) \leq 0.6c/(2\pi a) = 119.9$ THz.
Let us emphasize that this localized solution for the DCs embedded in the SCM can be obtained only if one extra cylinder is inserted. If we remove the extra cylinder from 2D lattice of the DCs in the SCM, the corresponding wave equation will be represented by adding the term $-(\epsilon - \varepsilon(\omega))\eta(\xi - |\mathbf{r} - \mathbf{r}_0|)E_z(x,y)$ to the right-hand side of Eq. (2). This term results in the positive potential in the effective 2D Schrödinger-type equation. This positive potential does not lead to the localized eigenfunction. Therefore, removed DC in the 2D ideal photonic crystal in the lattice of DCs embedded in the SCM does not result in the localized photonic mode causing the anomalous transmission.
Let us mention that the localization of the photonic mode at the frequency given by Eqs. (11) causes the anomalous infrared transmission inside the forbidden photonic band of the ideal photonic crystal. This allows us to use the SCCs in the DM and DC in the SCM with the symmetry broken by a defect as the infrared monochromatic filter.
Based on the results of our calculations we can conclude that it is possible to obtain a different type of a infrared monochromatic filter constructed as real photonic crystal formed by the SCCs embedded in DM and DCs embedded in SCM. The symmetry in these two systems can be broken by the defect of these photonic crystal, constructed by removing one cylinder out of the node of the ideal photonic crystal lattice and by inserting the extra cylinder, respectively, in other words, by making the "2D vacancy" and "2D interstitial" in the ideal photonic crystal lattice, respectively. Finally, we can conclude that the symmetry breaking resulting in the breakup of spacial periodicity of the dielectric function by removal of the SCC from periodic structure of SCCs embedded in DM, or inserting extra DC in SCM results in transmitted infrared frequency in the forbidden photonic band.

4.3 Far infrared monochromatic transmission through a film of type-II superconductor in magnetic field

Let us consider a system of Abrikosov vortices in a type-II superconductor that are arranged in a triangular lattice. We treat Abrikosov vortices in a superconductor as the parallel cylinders of the normal metal phase in the superconducting medium. The axes of the vortices, which are directed along the $\hat{z}$ axis, are perpendicular to the surface of the superconductor. We assume the $\hat{x}$ and $\hat{y}$ axes to be parallel to the two real-space lattice vectors that characterize the 2D triangular lattice of Abrikosov vortices in the film and the angle between $\hat{x}$ and $\hat{y}$ is equal $\pi/3$. The nodes of the 2D triangular lattice of Abrikosov vortices are assumed to be situated on the $\hat{x}$ and $\hat{y}$ axes.
For simplicity, we consider the superconductor in the London approximation (Abrikosov, 1988) i.e. assuming that the London penetration depth λ of the bulk superconductor is much greater than the coherence length ξ: $\lambda \gg \xi$. Here the London penetration depth is $\lambda = [m_e c^2/(4\pi n_e e^2)]^{1/2}$, where n_e is electron density. The coherence length is defined as $\xi = c/(\omega_{p0}\sqrt{\epsilon})$, where $\omega_{p0} = 2\pi c\omega_0$ is the plasma frequency. A schematic diagram of Abrikosov lattices in type-II superconductors is shown in Fig. 6 As it is seen from Fig. 6 the Abrikosov vortices of radius ξ arrange themselves into a 2D triangular lattice with lattice spacing $a(B,T) = 2\xi(T)\left[\pi B_{c2}/(\sqrt{3}B)\right]^{1/2}$ (Takeda et al., 2004) at the fixed magnetic field B and temperature T. Here B_{c2} is the critical magnetic field for the superconductor. We assume the wavevector of the incident electromagnetic wave vector $\mathbf{k}_i$ to be perpendicular to the direction of the Abrikosov vortices and the transmitted wave can be detected by using the detector D.

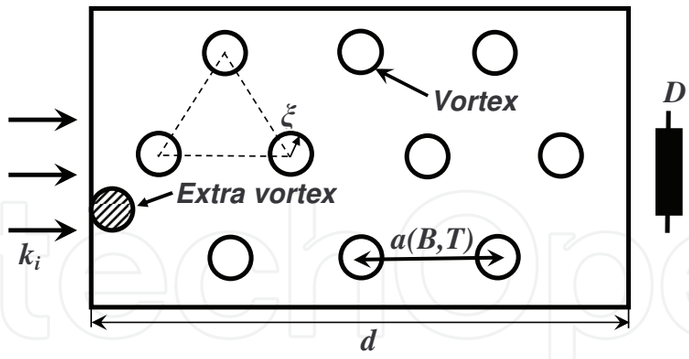

Fig. 6. Anomalous far infrared monochromatic transmission through a film of type-II superconductor in the magnetic field parallel to the vortices. $a(B,T)$ is the equilateral triangular Abrikosov lattice spacing. ξ is the coherence length and the radius of the vortex. d denotes the length of the film. The shaded extra vortex placed near the boundary of the film and situated outside of the node of the lattice denotes the defect of the Abrikosov lattice.

Now let us follow the procedure used in Ref. (Berman et al., 2006; 2008) to obtain the wave equation for Abrikosov lattice treated as a two-component photonic crystal. In Ref. (Berman et al., 2006), a system consisting of superconducting cylinders in vacuum is studied. By contrast, the system under study in the present manuscript consists of the cylindrical vortices in a superconductor, which is a complementary case (inverse structure) to what was treated in Ref. (Berman et al., 2006). For this system of the cylindrical vortices in the superconductor, we write the wave equation for the electric field $\mathbf{E}(x,y,t)$ parallel to the vortices in the form of 2D partial differential equation. The corresponding wave equation for the electric field is

$$-\nabla^2\mathbf{E} = -\frac{1}{c^2}\epsilon \sum_{\{\mathbf{n}^{(l)}\}} \eta(\mathbf{r})\frac{\partial^2\mathbf{E}}{\partial t^2} - \frac{4\pi}{c^2}\frac{\partial\mathbf{J}(\mathbf{r})}{\partial t}, \tag{13}$$

where ϵ is a dielectric constant of the normal metal component inside the vortices, $\eta(\mathbf{r})$ is the Heaviside step function which is $\eta(\mathbf{r}) = 1$ inside of the vortices and otherwise $\eta(\mathbf{r}) = 0$. In Eq. (13) $\mathbf{n}^{(l)}$ is a vector of integers that gives the location of a scatterer l at $\mathbf{a}(\mathbf{n}^{(l)}) \equiv \sum_{i=1}^{d} n_i^{(l)}\mathbf{a}_i$ ($\mathbf{a}_i$ are real space lattice vectors situated in the nodes of the 2D triangular lattice and d is the dimension of Abrikosov lattice).
At $(T_c - T)/T_c \ll 1$ and $\hbar\omega \ll \Delta \ll T_c$, where T_c is the critical temperature and Δ is the superconducting gap, a simple relation for the current density holds (Abrikosov, 1988):

$$\mathbf{J}(\mathbf{r}) = \left[-\frac{c}{4\pi\delta_L^2} + \frac{i\omega\sigma}{c}\right]\mathbf{A}(\mathbf{r}). \tag{14}$$

In Eq. (14) σ is the conductivity of the normal metal component.
The important property determining the band structure of the photonic crystal is the dielectric constant. The dielectric constant, which depends on the frequency, inside and outside of the vortex is considered in the framework of the two-fluid model. For a normal metal phase inside of the vortex it is $\epsilon_{in}(\omega)$ and for a superconducting phase outside of the vortex it is $\epsilon_{out}(\omega)$ and can be described via a simple Drude model. Following Ref. (Takeda et al., 2004) the dielectric

constant can be written in the form:

$$\epsilon_{in}(\omega) = \epsilon, \qquad \epsilon_{out}(\omega) = \epsilon\left(1 - \frac{\omega_{p0}^2}{\omega^2}\right). \tag{15}$$

Eqs. (15) are obtained in Ref. (Takeda et al., 2004) from a phenomenological two-component fluid model by applying the following condition: $\omega_{pn} \ll \omega \ll \gamma$. Here ω_{pn} is the plasma frequency of normal conducting electrons, and γ is the damping term in the normal conducting states.
Let's neglect a damping in the superconductor. After that substituting Eq. (14) into Eq. (13), considering Eqs. (15) for the dielectric constant, and seeking a solution in the form with harmonic time variation of the electric field, i.e., $\mathbf{E}(\mathbf{r},t) = \mathbf{E}_0(\mathbf{r})e^{i\omega t}$, $\mathbf{E} = i\omega\mathbf{A}/c$, we finally obtain the following equation

$$-\nabla^2 E_z(x,y) = \frac{\omega^2\epsilon}{c^2}\left[1 - \frac{\omega_{p0}^2}{\omega^2} + \frac{\omega_{p0}^2}{\omega^2}\sum_{\{\mathbf{n}^{(l)}\}}\eta(\mathbf{r})\right]E_z(x,y)\,. \tag{16}$$

The summation in Eq. (16) goes over all lattice nodes characterizing positions of the Abrikosov vortices. Eq. (16) describes Abrikosov lattice as the two-component 2D photonic crystal. The first two terms within the bracket are associated to the superconducting medium, while the last term is related to vortices (normal metal phase). Here and below the system described by Eq. (16) will be defined as an ideal photonic crystal. The ideal photonic crystal based on the Abrikosov lattice in type-II superconductor was studied in Refs. (Takeda et al., 2004). The wave equation (16) describing the Abrikosov lattice has been solved in Ref. (Takeda et al., 2004) where the photonic band frequency spectrum $\omega = \omega(\mathbf{k})$ of the ideal photonic crystal of the vortices has been calculated.
Let us consider an extra Abrikosov vortex pinned by some defect in the type-II superconducting material, as shown in Fig. 6. This extra vortex contributes to the dielectric contrast by the adding the term $\epsilon\omega_{p0}^2/c^2\eta(\xi - |\mathbf{r} - \mathbf{r}_0|)E_z(x,y)$, where $\mathbf{r}_0$ points out the position of the extra vortex, to the r.h.s. in Eq. (16):

$$-\nabla^2 E_z(x,y) = \frac{\omega^2\epsilon}{c^2}\left[1 - \frac{\omega_{p0}^2}{\omega^2} + \frac{\omega_{p0}^2}{\omega^2}\sum_{\{\mathbf{n}^{(l)}\}}\eta(\mathbf{r}) + \frac{\omega_{p0}^2}{\omega^2}\eta(\xi - |\mathbf{r} - \mathbf{r}_0|)\right]E_z(x,y), \tag{17}$$

Eq. (17) describes the type-II superconducting medium with the extra Abrikosov vortex pinned by a defect in the superconductor. We define the photonic crystal implying an extra Abrikosov vortex pinned by a defect as a real photonic crystal and it is described by Eq. (17). The eigenfrequency ω of the localized photonic state due to the extra Abrikosov vortex pinned by a defect is obtained from Eq. (17) as (Berman et al., 2008)

$$\omega(x) = \left(\omega_{up}^4(x) - A(x)\right)^{1/4}, \tag{18}$$

where $x = B/B_{c2}$ and function $A(x)$ is given by

$$A(x) = \frac{16c^4k_0^2(x)}{3\epsilon^2\xi^2}\exp\left[-\frac{8k_0^2(x)c^4}{3\epsilon^2\omega_{up}^2(x)\xi^2\omega_{p0}^2}\right] \tag{19}$$

and $k_0(x)$ is defined below through the electric field of the lower and higher photonic bands of the ideal Abrikosov lattice.
The electric field $E_z(x,y)$ corresponding to this localized photonic mode can be obtained from Eq. (17) as (Berman et al., 2008)

$$E_z^{(00)}(\mathbf{r}) = \begin{cases} \tilde{C}_1, & |\mathbf{r}-\mathbf{r}_0| < \xi\,, \\ \tilde{C}_2 B(x), & |\mathbf{r}-\mathbf{r}_0| > \xi\,, \end{cases} \tag{20}$$

where the constants $\tilde{C}_1$ and $\tilde{C}_2$ can be obtained from the condition of the continuity of the function $E_z^{(00)}(\mathbf{r})$ and its derivative at the point $|\mathbf{r}-\mathbf{r}_0| = \xi$ and

$$B(x) = \log\left[\xi\left(|\mathbf{r}-\mathbf{r}_0|\times\right.\right. \\ \left.\left.\exp\left[-4k_0^2(x)c^4/\left(3\epsilon^2\left(\tilde{\Delta}^2(x)-\omega_{p0}^2\right)\xi^2\omega_{p0}^2\right)\right]\right)^{-1}\right]. \tag{21}$$

The function $k_0(x)$ is given as

$$k_0\delta_{\alpha\beta} = -i\left(\left[\int E_{zc0}^*(\mathbf{r})\nabla E_{zv0}(\mathbf{r})d^2r\right]_{cv\alpha}\right)_\beta, \tag{22}$$

where $E_{zc0}(\mathbf{r})$ and $E_{zv0}(\mathbf{r})$ are defined by the electric field of the up and down photonic bands of the ideal Abrikosov lattice. The exact value of k_0 can be calculated by substituting the electric field $E_{zc0}(\mathbf{r})$ and $E_{zv0}(\mathbf{r})$ from Ref. (Takeda et al., 2004). Applying the weak coupling model (Abrikosov, 1988) corresponding to the weak dielectric contrast between the vortices and the superconductive media $\omega_{p0}^2/\omega^2\left|\sum_{\{\mathbf{n}^{(l)}\}}\eta(\mathbf{r})-1\right| \ll 1$ we use the approximate estimation of k_0 in our calculations as $k_0(x) \approx 2\pi/a(x) = \pi\xi^{-1}\sqrt{\sqrt{3}x/\pi}$.
We consider the Abrikosov lattice formed in the YBCO and study the dependence of the photonic band structure on the magnetic field. For the YBCO the characteristic critical magnetic field $B_{c2} = 5$ T at temperature $T = 85$ K is determined experimentally in Ref. (Safar et al., 1994). So we obtained the frequency corresponding to the localized wave for the YBCO in the magnetic field range from $B = 0.72B_{c2} = 3.6$ T up to $B = 0.85B_{c2} = 4.25$ T at $T = 85$ K. Following Ref. (Takeda et al., 2004), in our calculations we use the estimation $\epsilon = 10$ inside the vortices and for the YBCO $\omega_0/c = 77$ cm^{-1}. The dielectric contrast between the normal phase in the core of the Abrikosov vortex and the superconducting phase given by Eq. (15) is valid only for the frequencies below ω_{c1}: $\omega < \omega_{c1}$, where $\omega_{c1} = 2\Delta_S/(2\pi\hbar)$, $\Delta_S = 1.76k_BT_c$ is the superconducting gap, k_B is the Boltzmann constant, and T_c is the critical temperature. For the YBCO we have $T_c = 90$ K, and $\omega < \omega_{c1} = 6.601$ THz. It can be seen from Eqs. (18) and (20), that there is a photonic state localized on the extra Abrikosov vortex, since the discrete eigenfrequency corresponds to the electric field decreasing as logarithm of the distance from an extra vortex. This logarithmical behavior of the electric field follows from the fact that it comes from the solution of 2D Dirac equation. The calculations of the eigenfrequency ω dependence on the ratio B/B_{c2}, where B_{c2} is the critical magnetic field, is presented in Fig. 7. According to Fig. 7, our expectation that the the eigenfrequency level ω corresponding to the extra vortex is situated inside the photonic band gap is true. We calculated the frequency corresponding to the localized mode, which satisfies to the condition of the validity of the dielectric contrast given by Eq. (15). According to Eqs. (20) and (21), the localized field is decreasing proportionally to $\log\xi|\mathbf{r}-\mathbf{r}_0|^{-1}$ as the distance from an extra vortex increases. Therefore, in order to detect this localized mode, the length of the film d

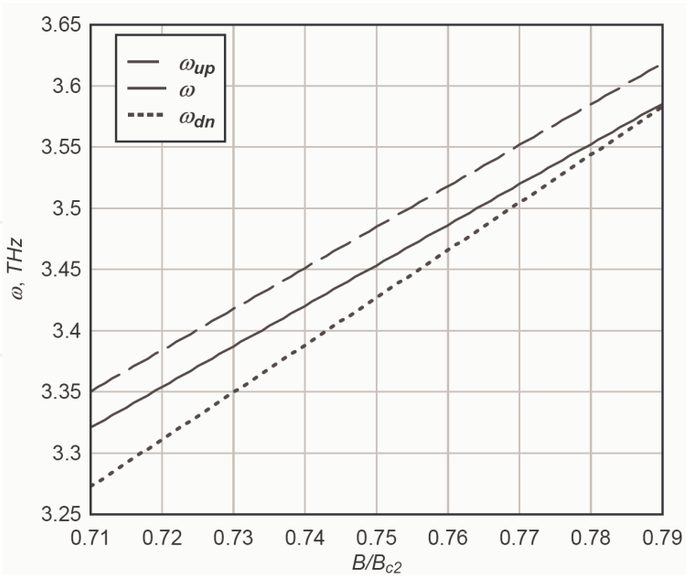

Fig. 7. The dependence of the photonic band structure of the real Abrikosov lattice on B/B_{c2}. Solid line represents the eigenfrequency ω corresponding to the localized mode near the extra vortex in the real Abrikosov lattice given by Eq. (18). The dashed and dotted lines represent, respectively, the top ω_{up} and bottom ω_{dn} boundaries of the photonic band gap of the ideal Abrikosov lattice according to Ref. (Takeda et al., 2004).

should not exceed approximately $10a(B/B_{c2})$, which corresponds to $d \lesssim 200$ μm for the range of magnetic fields for the YBCO presented by Fig. 7. For these magnetic fields $a \approx 20$ μm. Since the frequency corresponding to the localized mode is situated inside the photonic band gap, the extra vortex should be placed near the surface of the film as shown in Fig. 6. Otherwise, the electromagnetic wave cannot reach this extra vortex. Besides, we assume that this localized photonic state is situated outside the one-dimensional band of the surface states of two-dimensional photonic crystal. It should be mentioned, that in a case of several extra vortices separated at the distance greater than the size of one vortex (it is the coherence length estimated for the YBCO by $\xi \approx 6.5$ μm) the localized mode frequency for the both vortices is also going to be determined by Eq. (18). The intensity of the localized mode in the latter case is going to be enhanced due to the superposition of the modes localized by the different vortices. In the case of far separated extra vortices we have neglected by the vortex-vortex interaction. Thus, the existence of other pinned by crystal defects vortices increases the intensity of the transmitted mode and improves the possibility of this signal detection. Note that at the frequencies ω inside the photonic band gap $\omega_{dn} < \omega < \omega_{up}$ the transmittance and reflectance of electromagnetic waves would be close to zero and one, correspondingly, everywhere except the resonant frequency ω related to an extra vortex. The calculation of the transmittance and reflectance of electromagnetic waves at this resonant frequency ω is a very interesting problem, which will be analyzed elsewhere.

We considered a type-II superconducting medium with an extra Abricosov vortex pinned by a defect in a superconductor. The discrete photonic eigenfrequency corresponding to the localized photonic mode, is calculated as a function of the ratio B/B_{c2}, which parametrically depends on temperature. This photonic frequency increases as the ratio B/B_{c2} and temperature T increase. Moreover, since the localized field and the corresponding

photonic eigenfrequency depend on the distance between the nearest Abrikosov vortices $a(B,T)$, the resonant properties of the system can be tuned by control of the external magnetic field B and temperature T. Based on the results of our calculations we can conclude that it is possible to obtain a new type of a tunable far infrared monochromatic filter consisting of extra vortices placed out of the nodes of the ideal Abrikosov lattice, which can be considered as real photonic crystals. These extra vortices are pinned by a crystal defects in a type-II superconductor in strong magnetic field. As a result of change of an external magnetic field B and temperature T the resonant transmitted frequencies can be controlled.

5. Graphene-based photonic crystal

A novel type of 2D electron system was experimentally observed in graphene, which is a 2D honeycomb lattice of the carbon atoms that form the basic planar structure in graphite (Novoselov et al., 2004; Luk'yanchuk & Kopelevich, 2004; Zhang et al., 2005). Due to unusual properties of the band structure, electronic properties of graphene became the object of many recent experimental and theoretical studies (Novoselov et al., 2004; Luk'yanchuk & Kopelevich, 2004; Zhang et al., 2005; Novoselov et al., 2005; Zhang et al., 2005; Kechezhdi et al., 2008; Katsnelson, 2008; Castro Neto et al., 2009). Graphene is a gapless semiconductor with massless electrons and holes which have been described as Dirac-fermions (Novoselov et al., 2004; Luk'yanchuk & Kopelevich, 2004; Das Sarma et al., 2007). The unique electronic properties of graphene in a magnetic field have been studied recently (Nomura & MacDonald, 2006; Tőke et al., 2006; Gusynin & Sharapov, 2005;?). It was shown that in infrared and at larger wavelengths transparency of graphene is defined by the fine structure constant (Nair et al., 2008). Thus, graphene has unique optical properties. The space-time dispersion of graphene conductivity was analyzed in Ref. (Falkovsky & Varlamov, 2007) and the optical properties of graphene were studied in Refs. (Falkovsky & Pershoguba, 2007; Falkovsky, 2008).

In this Section, we consider a 2D photonic crystal formed by stacks of periodically placed graphene discs embedded into the dielectric film proposed in Ref. (Berman et al., 2010). The stack is formed by graphene discs placed one on top of another separated by the dielectric placed between them as shown in Fig. 8. We calculate the photonic band structure and transmittance of this graphene-based photonic crystal. We will show that the graphene-based photonic crystals can be applied for the devices for the far infrared region of spectrum.

Let us consider polarized electromagnetic waves with the electric field $\mathbf{E}$ parallel to the graphene discs. The wave equation for the electric field in a dielectric media has the form (Landau & Lifshitz, 1984)

$$-\triangle\mathbf{E}(\mathbf{r},t)+\nabla(\nabla\cdot\mathbf{E}(\mathbf{r},t))-\frac{\varepsilon(\mathbf{r})}{c^2}\frac{\partial^2\mathbf{E}(\mathbf{r},t)}{\partial t^2}=0\,, \tag{23}$$

where $\varepsilon(\mathbf{r},t)$ is the dielectric constant of the media.

In photonic crystals, dielectric susceptibility is a periodical function and it can be expanded in the Fourier series:

$$\varepsilon(\mathbf{r})=\sum_{\mathbf{G}}\varepsilon(\mathbf{G})e^{i\mathbf{G}\mathbf{r}}\,, \tag{24}$$

where $\mathbf{G}$ is the reciprocal photonic lattice vector.

Expanding the electric field on the Bloch waves inside a photonic crystal, and seeking solutions with harmonic time variation of the electric field, i.e., $\mathbf{E}(\mathbf{r},t)=\mathbf{E}(\mathbf{r})e^{i\omega t}$, one obtains

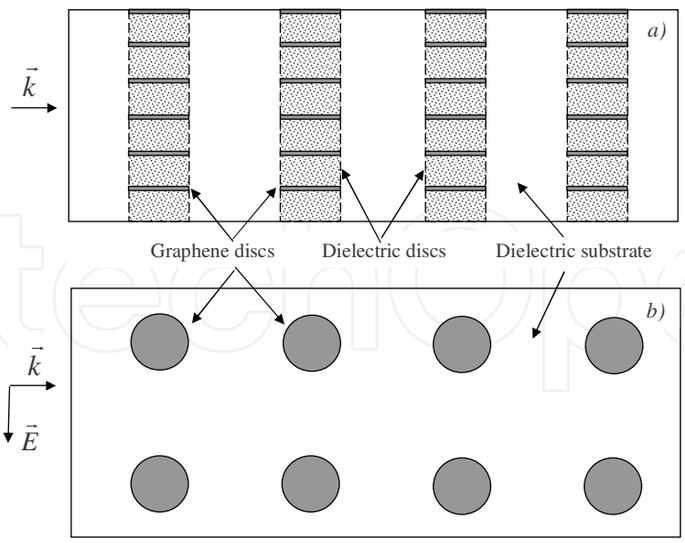

Fig. 8. Graphene-based photonic crystal: a) the side view. The material of the dielectric between graphene discs can be the same as the material of the dielectric substrate; b) the top view.

from Eq. (23) using Eq. (24) the system of equations for Fourier components of the electric field (Joannopoulos et al., 2008; McGurn & Maradudin, 1993):

$$(\mathbf{k}+\mathbf{G})^2 E_{\mathbf{k}}(\mathbf{G}) = \frac{\omega^2(\mathbf{k})}{c^2} \sum_{\mathbf{G}'} \varepsilon(\mathbf{G}-\mathbf{G}') E_{\mathbf{k}}(\mathbf{G}') \,, \tag{25}$$

which presents the eigenvalue problem for finding photon dispersion curves $\omega(\mathbf{k})$. In Eq. (25) the coefficients of the Fourier expansion for the dielectric constant are given by

$$\varepsilon(\mathbf{G}-\mathbf{G}') = \varepsilon_0 \delta_{\mathbf{G}\mathbf{G}'} + (\varepsilon_1 - \varepsilon_0) M_{\mathbf{G}\mathbf{G}'} \,. \tag{26}$$

In Eq. (26) ε_0 is the dielectric constant of the dielectric, ε_1 is the dielectric constant of graphene multilayers separated by the dielectric material, and $M_{\mathbf{G}\mathbf{G}'}$ for the geometry considered above is

$$\begin{aligned} M_{\mathbf{G}\mathbf{G}'} &= 2f \frac{J_1(|\mathbf{G}-\mathbf{G}'|r)}{(|\mathbf{G}-\mathbf{G}'|r)} \,, \quad \mathbf{G} \neq \mathbf{G}' \,, \\ M_{\mathbf{G}\mathbf{G}'} &= f \,, \quad \mathbf{G} = \mathbf{G}' \,, \end{aligned} \tag{27}$$

where J_1 is the Bessel function of the first order, and $f = S_g/S$ is the filling factor of 2D photonic crystal.

In our consideration the size of the graphene discs was assumed to be much larger than the period of the graphene lattice, and we applied the expressions for the dielectric constant of the infinite graphene layer for the graphene discs, neglecting the effects related to their finite size.

The dielectric constant $\varepsilon_1(\omega)$ of graphene multilayers system separated by the dielectric layers with the dielectric constant ε_0 and the thickness d is given by (Falkovsky & Pershoguba, 2007;

Falkovsky, 2008)

$$\varepsilon_1(\omega) = \varepsilon_0 + \frac{4\pi i \sigma_g(\omega)}{\omega d} \,, \tag{28}$$

where $\sigma_g(\omega)$ is the dynamical conductivity of the doped graphene for the high frequencies ($\omega \gg k v_F$, $\omega \gg \tau^{-1}$) at temperature T given by (Falkovsky & Pershoguba, 2007; Falkovsky, 2008)

$$\begin{aligned} \sigma_g(\omega) = \frac{e^2}{4\hbar} [\eta(\hbar\omega - 2\mu) \\ + \frac{i}{2\pi} \left(\frac{16 k_B T}{\hbar\omega} \log \left[2\cosh\left(\frac{\mu}{2k_B T} \right) \right] \right. \\ \left. - \log \frac{(\hbar\omega + 2\mu)^2}{(\hbar\omega - 2\mu)^2 + (2k_B T)^2} \right) \Bigg] \,. \end{aligned} \tag{29}$$

Here τ^{-1} is the electron collision rate, k is the wavevector, $v_F = 10^8$ cm/s is the Fermi velocity of electrons in graphene (Falkovsky, 2008), and μ is the the chemical potential determined by the electron concentration $n_0 = (\mu/(\hbar v_F))^2/\pi$, which is controlled by the doping. The chemical potential can be calculated as $\mu = (\pi n_0)^{1/2} \hbar v_F$. In the calculations below we assume $n_0 = 10^{11}$ cm^{-2}. For simplicity, we assume that the dielectric material is the same for the dielectric discs between the graphene disks and between the stacks. As the dielectric material we consider SiO_2 with the dielectric constant $\varepsilon_0 = 4.5$.

To illustrate the effect let us, for example, consider the 2D square lattice formed by the graphene based metamaterial embedded in the dielectric. The photonic band structure for the graphene based 2D photonic crystal with the array of cylinders arranged in a square lattice with the filling factor $f = 0.3927$ is presented in Fig. 9. The cylinders consist of the metamaterial stacks of alternating graphene and dielectric discs. The period of photonic crystal is $a = 25$ μm, the diameter of discs is $D = 12.5$ μm, the width of the dielectric layers $d = 10^{-3}$ μm . Thus the lattice frequency is $\omega_a = 2\pi c/a = 7.54 \times 10^{13}$ rad/s. The results of the plane wave calculation for the graphene based photonic crystal are shown in Fig. 9, and the transmittance spectrum obtained using the Finite-Difference Time-Domain (FDTD) method (Taflove, 1995) is presented in Fig. 10. Let us mention that plane wave computation has been made for extended photonic crystal, and FDTD calculation of the transmittance have been performed for five graphene layers. A band gap is clearly apparent in the frequency range $0 < \omega < 0.6$ and $0.75 < \omega < 0.95$ in units of $2\pi c/a$. The first gap is originated from the electronic structure of the doped graphene, which prevents absorbtion at $\hbar\omega < 2\mu$ (see also Eq. (29)). The photonic crystal structure manifests itself in the dependence of the lower photonic band on the wave vector k. In contrast, the second gap $0.75 < \omega < 0.95$ is caused by the photonic crystal structure and dielectric contrast.

According to Fig. 10, the transmittance T is almost zero for the frequency lower than $0.6\omega_a$, which corresponds to the first band gap shown in Fig. 9. The second gap in Fig. 9 (at the point G) corresponds to $\omega = 0.89\omega_a$, and it also corresponds to the transmittance spectrum minimum on Fig. 10.

Let us mention that at $\hbar\omega < 2\mu$ the dissipation of the electromagnetic wave in graphene is suppressed. In the long wavelength (low frequency) limit, the skin penetration depth is given by $\delta_0(\omega) = c/Re\left[2\pi\omega\sigma_g(\omega)\right]^{1/2}$ (Landau & Lifshitz, 1984). According to Eq. (29), $Re[\sigma_g(\omega < 2\mu)] = 0$, therefore, $\delta_0(\omega) \to +\infty$, and the electromagnetic wave penetrates along the graphene

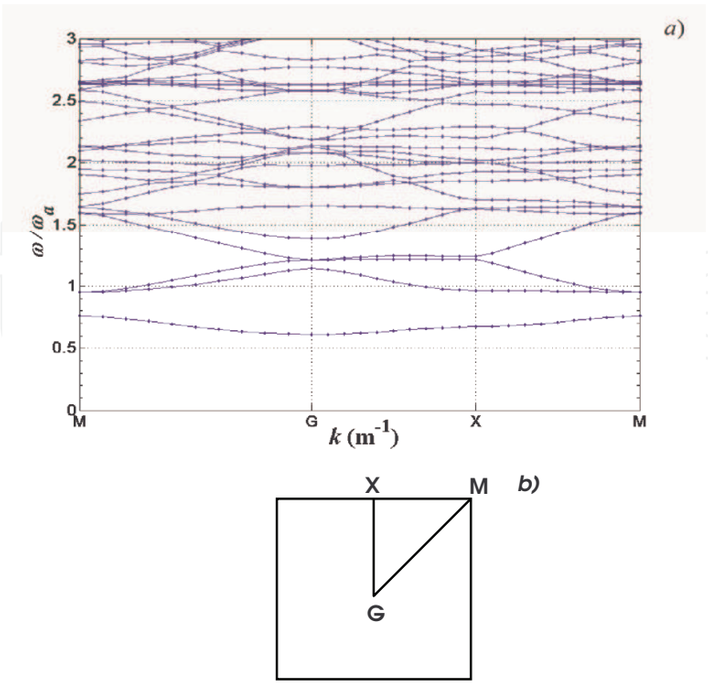

Fig. 9. a) Band structure of graphene based 2D square photonic crystal of cylinder array arranged in a square lattice. The cylinders consist of stack of graphene monolayer discs separated by the dielectric discs. The filling factor $f = 0.3927$. M, G, X, M are points of symmetry in the first (square) Brillouin zone. b) The first Brillouin zone of the 2D photonic crystal.

layer without damping. For the carrier densities $n_0 = 10^{11}$ cm^{-2} the chemical potential is $\mu = 0.022$ eV (Falkovsky & Pershoguba, 2007), and for the frequencies $\nu < \nu_0 = 10.42$ THz we have $Re[\sigma_g(\omega)] = 0$ at $\omega \gg 1/\tau$ the electromagnetic wave penetrates along the graphene

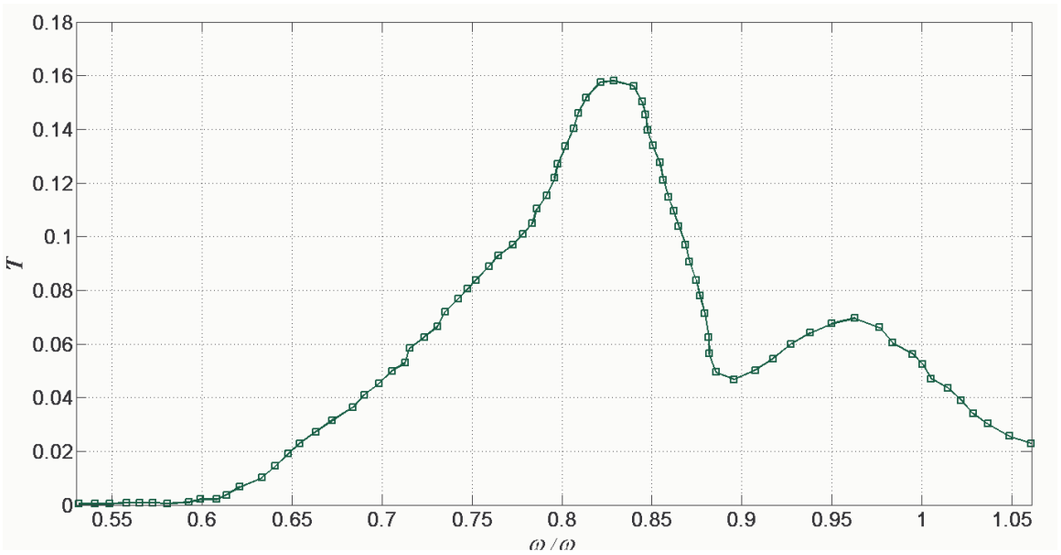

Fig. 10. The transmittance T spectrum of graphene based 2D photonic crystal.

layer almost without damping, which makes the graphene multilayer based photonic crystal to be distinguished from the metallic photonic crystal, where the electromagnetic wave is essentially damped. As a result, the graphene-based photonic crystals can have the sizes much larger than the metallic photonic crystals. The scattering of the electrons on the impurities can result in non-zero $Re[\sigma_g(\omega)]$, which can cause the dissipation of the electromagnetic wave. Since the electron mobility in graphene can be much higher than in typical semiconductors, one can expect that the scattering of the electrons on the impurities does not change the results significantly.

The physical properties of graphene-based photonic crystals are different from the physical properties of other types of photonic crystals, since the dielectric constant of graphene has the unique frequency dependence (Falkovsky & Pershoguba, 2007; Falkovsky, 2008). According to the results presented above, the graphene-based photonic crystal has completely different photonic band structure in comparison to the photonic crystals based on the other materials. The photonic band structure of the photonic crystal with graphene multilayer can be tuned by changing the distance d between graphene discs in the r.h.s. of Eq. (28). The photonic band structure of the graphene-based photonic crystals can also be controlled by the doping, which determines the chemical potential μ entering the expressions for the conductivity and dielectric constant of graphene multilayer (29).

6. Discussion and conclusions

Comparing the photonic band structure for graphene-based photonic crystal presented in Fig. 9 with the dielectric (Joannopoulos et al., 2008), metallic (McGurn & Maradudin, 1993; Kuzmiak & Maradudin, 1997), semiconductor (McGurn & Maradudin, 1993) and superconductor-based (Berman et al., 2006; Lozovik et al., 2007) photonic crystals, we conclude that only graphene- and superconductor-based photonic crystals have essential photonic band gap at low frequencies starting $\omega = 0$, and the manifestation of the gap in the transmittance spectra is almost not suppressed by the damping effects. Therefore, only graphene-based and superconducting photonic crystals can be used effectively as the frequency filters and waveguides in low-frequency for the far infrared region of spectrum, while the devices based on the dielectric photonic crystals can be used only in the optical region of electromagnetic waves spectrum. The graphene based-photonic crystal can be used at room temperatures, while the superconductor-based photonic crystal can be used only at low temperatures below the critical temperature T_c, which is about 90 K for the YBCO superconductors.

In summary, photonic crystals are artificial media with a spatially periodical dielectric function. Photonic crystals can be used, for example, as the optical filters and waveguides. The dielectric- and metal-based photonic crystals have different photonic bands and transmittance spectrum. It was shown that the photonic band structure of superconducting photonic crystal leads to their applications as optical filters for far infrared frequencies . It is known that the dielectric- and metal-based photonnic crystals with defects can be used as the waveguides for the frequencies corresponding to the media forming the photonic crystals. Far infrared monochromatic transmission across a lattice of Abrikosov vortices with defects in a type-II superconducting film is predicted. The transmitted frequency corresponds to the photonic mode localized by the defects of the Abrokosov lattice. These defects are formed by extra vortices placed out of the nodes of the ideal Abrokosov lattice. The extra vortices can be pinned by crystal lattice defects of a superconductor. The corresponding frequency is studied as a function of magnetic field and temperature. The control of the transmitted

frequency by varying magnetic field and/or temperature is analyzed. It is suggested that found transmitted localized mode can be utilized in the far infrared monochromatic filters. Besides, infrared monochromatic transmission through a superconducting multiple conductor system consisting of parallel superconducting cylinders is found. The transmitted frequency corresponds to the localized photonic mode in the forbidden photonic band, when one superconducting cylinder is removed from the node of the ideal two-dimensional lattice of superconducting cylinders. A novel type of photonic crystal formed by embedding a periodic array of constituent stacks of alternating graphene and dielectric discs into a background dielectric medium is proposed. The frequency band structure of a 2D photonic crystal with the square lattice of the metamaterial stacks of the alternating graphene and dielectric discs is obtained. The electromagnetic wave transmittance of such photonic crystal is calculated. The graphene-based photonic crystals have the following advantages that distinguish them from the other types of photonic crystals. They can be used as the frequency filters for the far-infrared region of spectrum at the wide range of the temperatures including the room temperatures. The photonic band structure of the graphene-based photonic crystals can be controlled by changing the thickness of the dielectric layers between the graphene discs and by the doping. The sizes of the graphene-based photonic crystals can be much larger than the sizes of metallic photonic crystals due to the small dissipation of the electromagnetic wave. The graphene-based photonic crystals can be used effectively as the frequency filters and waveguides for the far infrared region of electromagnetic spectrum. Let us also mention that above for simplicity we assume that the dielectric material is the same between the graphene disks and between the stacks. This assumption has some technological advantage for the most easier possible experimental realization of the graphene-based photonic crystal.

7. References

Abrikosov, A. A. (1988). *Fundamentals of the Theory of Metals* (North Holland, Amsterdam).

Berman, O. L., Boyko, V. S., Kezerashvili, R. Ya., and Lozovik, Yu .E. (2008). Anomalous far-infrared monochromatic transmission through a film of type-II superconductor in magnetic field. *P*hys. Rev. B, 78, 094506.

Berman, O. L., Boyko, V. S., Kezerashvili, R. Ya., and Lozovik, Yu .E. (2009). Monochromatic Infrared Wave Propagation in 2D Superconductor−Dielectric Photonic Crystal. *L*aser Physics, 19, No. 10, pp. 2035−2040.

Berman, O. L., Boyko, V. S., Kezerashvili, R. Ya., Kolesnikov, A. A., and Lozovik, Yu .E. (2010). Graphene-based photonic crystal. *P*hysics Letters A, 374, pp. 4784−4786.

Berman, O. L., Lozovik, Yu. E., Eiderman, S. L., and Coalson, R. D. (2006). Superconducting photonic crystals: Numerical calculations of the band structure. *P*hys. Rev. B, 74, 092505.

Castro Neto, A. H., Guinea, F.,, Peres, N. M. R., Novoselov, K. S. and Geim, A. K. (2009). The electronic properties of graphene, *R*eviews of Modern Physics, 81, pp. 109–162.

Chigrin, D. N. and Sotomayor Torres, C. M.. (2003). Self-guiding in two-dimensional photonic crystals. *O*ptics Express, 11, No 10, pp. 1203–1211.

Das Sarma, S., Hwang, E. H., and Tse, W. K. (2007). Many-body interaction effects in doped and undoped graphene: Fermi liquid versus non-Fermi liquid. *P*hys. Rev. B, 75, 121406(R).

Falkovsky, L. A. and Pershoguba, S. S. (2007). Optical far-infrared properties of a graphene monolayer and multilayer. *P*hys. Rev. B, 76, 153410.

Falkovsky, L. A. and Varlamov, A A. (2007). Space-time dispersion of graphene conductivity.

*E*ur. Phys. J. B 56, pp. 281–284.
Falkovsky, L. A. (2008). Optical properties of graphene. *J*. Phys.: Conf. Ser., 129, 012004.
Gusynin, V. P. and Sharapov, S. G. (2005). Magnetic oscillations in planar systems with the Dirac-like spectrum of quasiparticle excitations. II. Transport properties, *P*hys. Rev. B, 71, 125124.
Gusynin, V. P. and Sharapov, S. G. (2005). Unconventional Integer Quantum Hall Effect in Graphene, Phys. Rev. Lett., 95, 146801.
Joannopoulos, J. D., Meade, R. D., and Winn, J. N. (1995). *Photonic Crystals: The Road from Theory to Practice* (Princeton University Press, Princeton, NJ).
Joannopoulos, J. D., Johnson, S. G., Winn, J. N., and Meade, R. D. (2008). *Photonic Crystals: Molding the Flow of Light* (Second Edition, Princeton University Press, Princeton, NJ).
John, S. (1987). Strong localization of photons in certain disordered dielectric superlattices. *P*hys. Rev. Lett., 58, pp. 2486–2489.
Katsnelson, M. I. (2008). Optical properties of graphene: The Fermi liquid approach. *E*urophys. Lett., 84, 37001.
Kechedzhi, K., Kashuba O., and Fal'ko, V. I. (2008). Quantum kinetic equation and universal conductance fluctuations in graphene. *P*hys. Rev. B, 77, 193403.
Keldysh, L. V. (1964). Deep levels in semiconductors. *S*ov. Phys. JETP 18, 253.
Kohn, W. (1957). In *Solid State Physics*, edited by F. Seitz and D. Turnbull, vol. 5, pp. 257–320 (Academic, New York).
Kuzmiak, V. and Maradudin, A. A. (1997). Photonic band structures of one- and two-dimensional periodic systems with metallic components in the presence of dissipation. *P*hys. Rev. B 55, pp. 7427–7444.
Landau. L. D. and Lifshitz, E. M. (1984). *Electrodynamics of continuous media.* (Second Edition, Pergamon Press, Oxford).
Lozovik, Yu. E., Eiderman, S. I., and Willander, M. (2007). The two-dimensional superconducting photonic crystal. *L*aser physics, 9, No 17, pp. 1183–1186.
Luk'yanchuk, I. A. and Kopelevich, Y. (2004). Phase Analysis of Quantum Oscillations in Graphite. *P*hys. Rev. Lett., 93, 166402.
Luttinger, J. M. and Kohn, W. (1955). Motion of Electrons and Holes in Perturbed Periodic Fields. *P*hys. Rev., 97, pp. 869–883.
McGurn, A. R. and Maradudin, A. A. (1993). Photonic band structures of two- and three-dimensional periodic metal or semiconductor arrays. *P*hys. Rev. B, 48, pp. 17576–17579.
Meade, R. D., Brommer, K. D., Rappe, A. M., and Joannopoulos, J. D. (1991). Photonic bound states in periodic dielectric materials. *P*hys. Rev. B, 44, pp. 13772–13774.
Meade, R. D., Brommer, K. D., Rappe, A. M. and Joannopoulos, J. D. (1992). Existence of a photonic band gap in two dimensions. *A*ppl. Phys. Lett., 61, pp. 495–497.
Meade, R. D., Rappe, A. M., Brommer K. D., Joannopoulos, J. D., and Alerhand, O. L. (1993). Accurate theoretical analysis of photonic band-gap materials. *P*hys. Rev. B 48, pp. 8434–8437.
McCall, S. L., Platzmann, P. M., Dalichaouch R., Smith, D. and Schultz, S. (1991). Microwave propagation in two-dimensional dielectric lattices. *P*hys. Rev. Lett. 67, pp. 2017–2020.
Nair, R. R., Blake, P., Grigorenko, A. N., Novoselov, K. S., Booth, T. J., Stauber, T., Peres, N. M. R., and Geim, A. K. (2008). Fine Structure Constant Defines Visual Transparency of Graphene. *S*cience, 320, no. 5881, 1308.
Nomura, K. and MacDonald, A. H. (2006). Quantum Hall Ferromagnetism in Graphene.

*P*hys. Rev. Lett., 96, 256602.

Novoselov, K. S., Geim, A. K., Morozov, S. V., Jiang, D., Zhang, Y., Dubonos, S. V., Grigorieva, I. V., and Firsov, A. A. (2004). Electric Field Effect in Atomically Thin Carbon Films. *S*cience, 306, no. 5696, pp. 666–669.

Novoselov, K. S., Geim, A. K., Morozov, S. V., Jiang, D., Katsnelson, M. I., Grigorieva, I. V. and Dubonos, S. V., (2005). Two-Dimensional Gas of Massless Dirac Fermions in Graphene. *N*ature (London), 438, pp. 197–200.

Robertson, W. M., Arjavalingam, G., Meade, R. D., Brommer, K. D., Rappe, A. M., and Joannopoulos, J. D. (1992). Measurement of photonic band structure in a two-dimensional periodic dielectric array, *P*hys. Rev. Lett., 68, pp. 2023–2026.

Safar, H., Gammel, P. L., Huse, D. A., Majumdar, S. N., Schneemeyer, L. F., Bishop, D. J., López, D., Nieva, G., and de la Cruz, F. (1994). Observation of a nonlocal conductivity in the mixed state of $YBa_2Cu_3O_{7-\delta}$: Experimental evidence for a vortex line liquid. *P*hys. Rev. Lett., 72, pp. 1272–1275.

Taflove, A. (1995). *Computational Electrodynamics: The Finite-Difference Time-Domain Method* (MA: Artech House).

Takeda, H. and Yoshino, K. (2003). Tunable light propagation in Y-shaped waveguides in two-dimensional photonic crystals utilizing liquid crystals as linear defects. *P*hys. Rev. B, 67, 073106.

Takeda, H. and Yoshino, K. (2003). Tunable photonic band schemes in two-dimensional photonic crystals composed of copper oxide high-temperature superconductors. *P*hys. Rev. B, 67, 245109.

Takeda, H., Yoshino, K., and Zakhidov, A. A. (2004). Properties of Abrikosov lattices as photonic crystals. *P*hys. Rev. B, 70, 085109.

Takhtamirov, E. E. and Volkov, V. A. (1999). Generalization of the effective mass method for semiconductor structures with atomically sharp heterojunctions. *J*ETP, 89, No 5, pp. 1000–1014.

Tőke, C., Lammert, P. E., Crespi, V. H., and Jain, J. K. (2006). Fractional quantum Hall effect in graphene. *P*hys. Rev. B, 74, 235417.

Yablonovitch, E. (1987). Inhibited Spontaneous Emission in Solid-State Physics and Electronics, *P*hys. Rev. Lett., 58, pp. 2059–2062.

Yablonovitch, E., Gmitter, T. J., Meade, R. D., Brommer, K. D., Rappe, A. M., and Joannopoulos, J. D. (1991). Donor and acceptor modes in photonic band structure. *P*hys. Rev. Lett., 67, pp. 3380–3383.

Zhang, Y., Small, J. P., Amori, M. E. S., and Kim P. (2005). Electric Field Modulation of Galvanomagnetic Properties of Mesoscopic Graphite. *P*hys. Rev. Lett., 94, 176803.

Zhang, Y., Tan, Y.-W., Stormer, H. L., and Kim, P. (2005). Experimental observation of the quantum Hall effect and Berry's phase in graphene. *N*ature, 438, pp. 201–204.

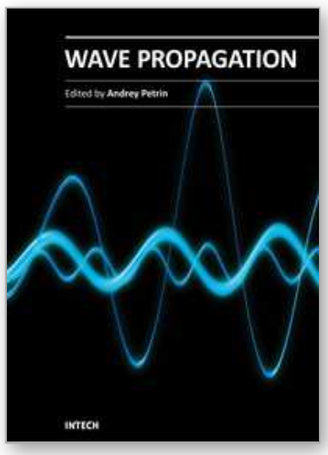

Wave Propagation
Edited by Dr. Andrey Petrin

ISBN 978-953-307-275-3
Hard cover, 570 pages
Publisher InTech
Published online 16, March, 2011
Published in print edition March, 2011

The book collects original and innovative research studies of the experienced and actively working scientists in the field of wave propagation which produced new methods in this area of research and obtained new and important results. Every chapter of this book is the result of the authors achieved in the particular field of research. The themes of the studies vary from investigation on modern applications such as metamaterials, photonic crystals and nanofocusing of light to the traditional engineering applications of electrodynamics such as antennas, waveguides and radar investigations.

How to reference
In order to correctly reference this scholarly work, feel free to copy and paste the following:

Oleg L. Berman, Vladimir S. Boyko, Roman Ya. Kezerashvili and Yurii E. Lozovik (2011). Electromagnetic Wave Propagation in Two-Dimensional Photonic Crystals, Wave Propagation, Dr. Andrey Petrin (Ed.), ISBN: 978-953-307-275-3, InTech, Available from: http://www.intechopen.com/books/wave-propagation/electromagnetic-wave-propagation-in-two-dimensional-photonic-crystals

INTECH
open science | open minds

InTech Europe
University Campus STeP Ri
Slavka Krautzeka 83/A
51000 Rijeka, Croatia
Phone: +385 (51) 770 447
Fax: +385 (51) 686 166
www.intechopen.com

InTech China
Unit 405, Office Block, Hotel Equatorial Shanghai
No.65, Yan An Road (West), Shanghai, 200040, China
中国上海市延安西路65号上海国际贵都大饭店办公楼405单元
Phone: +86-21-62489820
Fax: +86-21-62489821

IntechOpen